CANCOM2024 – CANADIAN INTERNATIONAL CONFERENCE ON COMPOSITE MATERIALS

# MORPHOLOGICALLY-ENGINEERED LASER-INDUCED GRAPHENE/PDMS STRETCHABLE SENSORS FOR LARGE DEFORMATION MEASUREMENT IN FABRIC REINFORCEMENTS

Amindehghan, Mohammad Amin, Seethaler, Rudolf*, and S. Milani, Abbas*

Composite Research Network-Okanagan Laboratory, School of Engineering, The University of British Columbia, Kelowna, Canada
* Corresponding authors (abbas.milani@ubc.ca, rudolf.seethaler@ubc.ca)

**Keywords**: *Woven fabric reinforcement, Stretchable strain sensors, Wrinkling*

## ABSTRACT

Accurately measuring strain under different deformation modes, such as shear, tensile, and bending, is crucial for evaluating textile composite reinforcements' performance in terms of defects like wrinkling during their forming processes. Conventional strain gauges or rigid fiber-shape strain sensors are impractical for this purpose, owing to the low shear and bending stiffness magnitudes of the reinforcement in dry conditions. This study presents a novel stretchable strain sensor based on laser-induced graphene/PDMS with a customized geometry. The sensor can be placed onto the textile fabric at any local point of sampling to measure deformation resulting from shear, tensile, or bending deformations. The sensor's performance was assessed through uniaxial tensile, bias extension, and a customized bending test, conducted on comingled glass fiber/polypropylene (PP) woven fabric specimens. The sensor could detect shear angles up to 50 degrees, tensile strain up to 3% and bending angle up to ±90 degree. A novel configuration of the sensors enabled us to differentiate between these loading modes.

## 1 INTRODUCTION

Woven fabric reinforced composites (WFRC) have attracted significant interest over the past decades owing to their superior mechanical properties and formability across various polymer composite applications such as those in aerospace, automotive, and energy sectors [1]. Forming WFRC involves preforming dry fabric followed by resin impregnation, or thermo-stamping in the case of the pre-impregnated plies [2]. However, these often lead to process-induced defects, particularly wrinkling, attributed to the low bending stiffness of the forming fabric when conformed to complex molds [3]. Essentially, wrinkles emerge when the compression force within the yarn surpasses the critical buckling load, resulting in out-of-plane deformation. This defect significantly impacts the final product's quality and is a primary focus of the current research. Another interacting source of wrinkling in woven fabrics is shear deformation beyond the shear locking angle, observable during bias extension and picture frame tests [2]. Many past studies have explored the numerical and experimental relationships between various parameters such as fabric geometrical and material characteristics, loading boundary conditions, and induced tension in the fabric, eventually aiming to develop reliable finite element models that can aid in predicting and mitigating wrinkling by adjusting the above forming parameters [3-6]. While numerical models have been instrumental in assessing the wrinkle formation in forming of WFRC, challenges remain in terms of precision, validation, and computational costs. The complexity of simulating 3D forming processes and limited access to

measurement devices may hinder the accurate identification and validation of meso-micro level finite element models. Traditional rigid strain sensors are inadequate due to the soft nature of fabrics, necessitating visual and non-contact measurement methods such as digital image correlation (DIC) [7]. Although DIC enhances measurement accuracy and characterization automation, particularly in forming processes, its requirement for stereo-DIC setups, visual access, and limitations in investigating wrinkling beneath the first layer of the layup pose significant challenges. Consequently, there exists a pressing need for more capable measurement systems to investigate fabrics deformation during the forming processes [8]. Incorporation of soft strain sensors on fabrics have been only recently reported in the studies [9, 10].

Following the above research trend, herein **we aim to develop soft sensors for woven fabrics characterization at dry level, specifically by developing and testing a piezoresistive stretchable strain sensor system based on nanocomposite of laser-induced graphene (LIG) and silicone elastomer polydimethylsiloxane (PDMS)**. We show how such a sensing system, with a customized geometry, enables local measurement of tensile, shear, and bending of the woven reinforcement. The sensor's morphologically-engineered sensor design facilitates identification and measurement of different fabric deformation modes, while its very low stiffness ensures minimal interference with the fabric's virgin behaviour.

# 2 EXPERIMENTAL

## *2.1 Test material and characterization modes*

Polyimide tape from Dupont (HN200) serves as the substrate for direct laser writing (DLW), while PDMS Sylgard 184 from Dow Corning acts as the matrix for the sensor. All experimentations were conducted on a TWINTEX® comingle glass fiber/polypropylene (PP) woven fabric. Scanning electron microscopy (SEM) imaging was performed using the MIRA 3 TESCAN scanning electron microscope. Uniaxial and bias-extension tests [9] were carried out utilizing an Instron 5960 Universal Test Machine, while bending tests were facilitated through a custom-made bending moment setup [11]. The resistance signals of the sensors are recorded using NI-9219 systems from National Instruments.

## *2.2 Sensor and sensing system design*

The ultimate motivation of this study has been to devise new sensor configurations capable of not only gauging the magnitude of applied loading in WFRC, but also discerning their types, be it tensile, shear, or bending. To achieve this, employing two distinct sensors (with the exact same design nature) on different locations of the fabric—one for shear and another for tensile/bending identification—can fulfil our objective. Moreover, each sensor adopts a twin-shaped design to facilitate load direction detection, thus enabling differentiation between tensile and bending loads (Figure 1 (a)). Each sensor comprises three structural components: two circular areas serving as electrode pads for substrate adhesion, and a central sensing area (Figure 1b). In this study, an S-shaped design was implemented within the sensing area to better accommodate the rotational movement of the fabric during shear deformation, ensuring a stable response, as will be shown in Section 3. Figure 1c depicts the configurations of the tensile and shear sensors devised.

## *2.3 Sensor fabrication*

The fabrication process of the sensor is shown in Figure 2. The process commences with a direct laser writing on the polyimide tape to synthesize Laser-Induced Graphene (LIG), utilizing an Oxford Micromachining UV laser with a 355 nm wavelength. Five adjustable parameters of the laser—power, speed, hatch distance (distance between parallel lines of laser), focal length, and frequency—were meticulously calibrated. After numerous experiments, optimal parameters for LIG synthesis were determined as detailed in Table 1. Initially, a large rectangular area (90 mm × 50 mm) was irradiated, as depicted in Figure 2 (a). Subsequently, a thin layer of PDMS (mixture of prepolymer and

hardener in a 10:1 ratio) with a thickness of 0.3 mm was applied onto the LIG area using a film applicator (Figure 2 (b)). The assembly was vacuumed for 15 minutes to eliminate bubbles and ensure complete infiltration of PDMS into the LIG structure. Following this, the sample was cured on a hot plate at 100°C for 1 hour. The subsequent step involved peeling off the PDMS/LIG from the Kapton tape, followed by shaping the sensors using the same laser with higher power to obtain the desired form. The material exhibited piezoresistive properties, meaning its electrical resistance alters upon the application of deformation. Finally, the sensor was affixed onto the fabric using silicone glue (Smooth-on), and electrodes were attached using silver paste onto electrode pads, as illustrated in Figure 1(c).

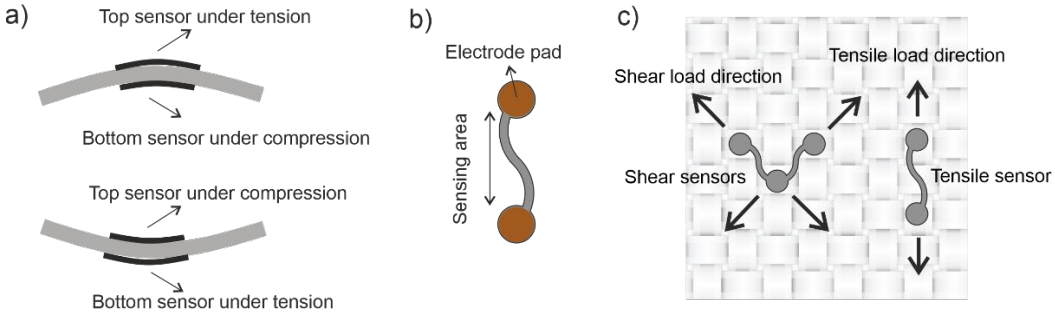


Figure 1 (a) Applied configuration of the new tensile sensor(s) for bending mode detection, (b) different parts of each sensor, (c) shape and arrangement of the sensors system applied to the tensile mode and shear mode detections.

Table I Optimized laser parameters for LIG synthesis.

| Laser Parameter | Power | Speed | Hatch | Frequency | Defocus |
|---|---|---|---|---|---|
| Value | 2.3 W | 50 mm/s | 0.05 mm | 40 kHz | +6 mm |

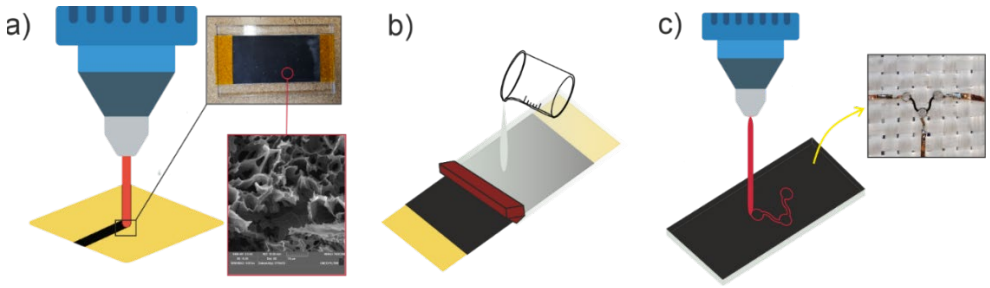


Figure 2 Overview of the new sensor fabrication. (a) Direct laser writing on polyimide tape; SEM image is shown in inset. (b) casting of PDMS on the LIG using film applicator.(c) cutting PDMS/LIG sensor in the desired shape for embedment onto fabric.

### *2.4 Data processing*

We conducted three mechanical tests: uniaxial tensile, shear bias-extension, and bending utilizing a customized setup [11]. For the tensile and bias-extension tests, the glass fiber/PP fabric was cut into a rectangular shape measuring 150 mm × 75 mm (length × width), while for the bending test, a rectangular sample of 20 mm × 40 mm was used. All tests were repeated four times to assess the repeatability of the sensors. The resistance signals of the sensors are expressed in normalized resistance to facilitate better comparison among different sensors,

$$R_{normalized} = \frac{R - R_0}{R_0} \quad (1)$$

Where, $R$ is the recorded electrical resistance of the sensor and $R_0$ is the initial resistance of the sensor before the test. Another term used in the measurements is the gauge factor (GF) which is an index of sensor sensitivity (as the ratio of normalized resistance to the applied strain ($\varepsilon$)). Shear angle in the center of the sample in the bias-extension

test can be analytically determined through Eq (2) [9], where, $\gamma$ is the shear angle, $L_0 = H - W$ and $H$ and $W$ is the original height and width of the sample.

$$\gamma = 90 - 2\cos^{-1}\left(\frac{L_0 + \delta}{\sqrt{2}L_0}\right) \quad (2)$$

# 3 RESULTS AND DISCUSSION

## *3.1 Tensile, shear and bending tests*

The performance assessment of the tensile and shear sensors was conducted through uniaxial and bias-extension tests, respectively. In Figure 3(a), the response of the tensile sensors (positioned on both sides of the fabric for comparisons) to the applied tensile force is illustrated. Both sensors exhibit an increase in resistance, albeit with different slopes; notably, the front sensor demonstrates a higher sensitivity to the applied load. The GF values for the front and back sensors are 16 and 6.67, respectively, which is quite a large variation and requires improvement in future work. Additionally, both sensors exhibit strong repeatability, with all four tests closely aligned. In Figure 3(b), the response of the shear sensors to the bias-extension test is depicted. The shear sensor on the left side, aligned with the load direction, experiences tension, while the right shear sensor is subjected to compression, as illustrated in Figure 3(c). This behavior is reflected in the sensor response, with the left shear sensor exhibiting a sharp increase in resistance, whereas the right sensor remains nearly unchanged. This performance enables the measurement and detection of the shear force direction by comparing the responses of each side of the shear sensors. Furthermore, both sensors demonstrate high repeatability, with the left sensor displaying a linear response up to a shear angle of 50 degrees, which proves beneficial for the calibration process. The bending response of the sensing system (using two tensile sensors per Figure 1a) is discussed in the next section.

## *3.2 A cross sensitivity evaluation: Confirming distinguishable sensing modes*

As mentioned in the previous section, differentiating between various loads becomes essential when an unknown or combination of loads are applied to the specimen. Therefore, we assessed the cross sensitivity of the tensile and shear sensors to loads other than their designated one. Figures 4(a) and 4(b) depict the response of the tensile and shear sensors to bias-extension and uniaxial tensile tests, respectively. While both sensors exhibit responses to these tests, their intensity and patterns differ. For instance, the front and back tensile sensors show only a small increase in normalized resistance, 0.085 and 0.022 respectively, which accounts for less than 17% of their response to the tensile load within the test range. Similarly, both shear sensors demonstrate an increase in normalized resistance up to 0.15, less than 5% of their response to shear load. Both sides of the shear sensor display resistance increases due to experiencing the same load. Another potential load during a forming process is the bending of the fabric, necessitating an evaluation of the sensors' responses. Figures 4(c) and 4(d) illustrate the response of the tensile and shear sensors to the bending cycle test, respectively. The bending cycle ranges from 0 to 90 degrees, 90 to -90, and -90 to 0. In Figure 4(c), when the sample bends at +90 degrees, the front sensor exhibits a substantial increase in resistance, whereas the back sensor shows less change. Conversely, at -90 degrees, the back sensor demonstrates an increase while the front sensor remains relatively stable. The above sensing system behavior aids in the discrimination between tensile and bending loads, as both sensors exhibit nearly identical increases in resistance during tensile tests (Figure 3(a)). The situation differs for the shear sensors (Figure 4(d)): since both sensors are on one side of the sample, they undergo the same tension/compression during a bending test. Hence, in one direction (-90 degrees), both sensors display significant resistance changes, while in +90 degrees, they remain relatively constant. These results indicate that both tensile and shear sensors are profoundly influenced by bending deformation, but in a predictable and distinct manner from the other tests. Consequently, by comparing the signals from all sensors, it becomes feasible to discern the applied load(s), their magnitude, and direction by the devices sensor system for each mode.

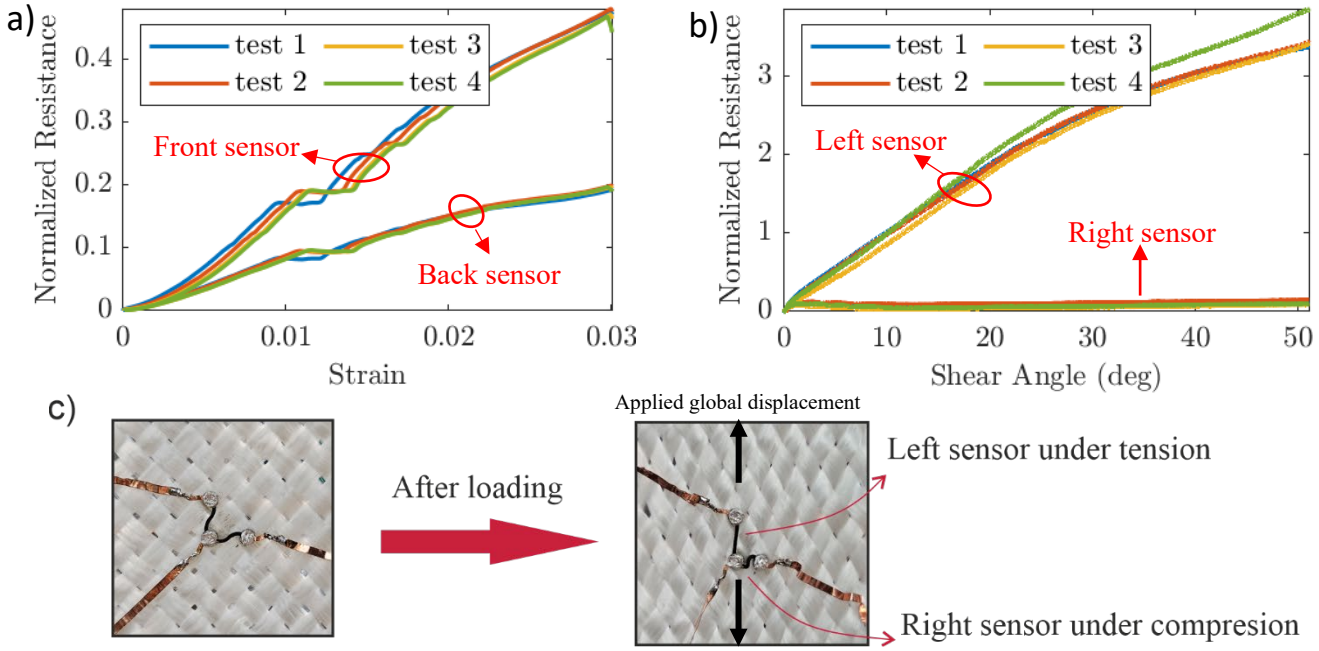


Figure 3 response of (a) tensile sensors to the uniaxial tensile test, (b) shear sensors to the bias-extension test. (c) shape of the shear sensors before and after bias-extension shear loading.

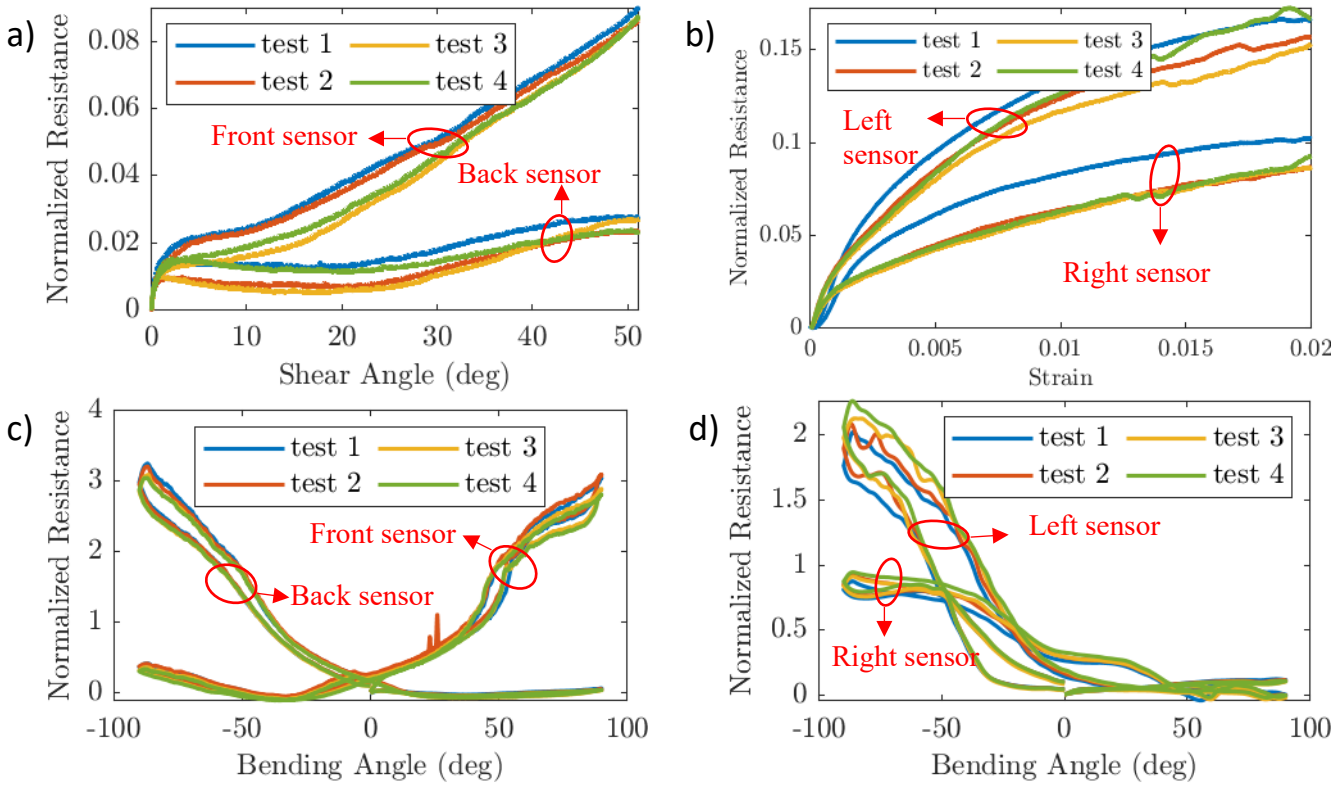


Figure 4 response of the (a) tensile sensors to shear deformation, (b) shear sensors to tensile test, (c) and (d) tensile sensors and shear sensors to bending test, respectively.

# 4 Conclusion

This study explored the integration of soft strain sensors onto woven fabric reinforcements to accurately detect and measure local tensile, shear, and bending deformations. We developed a nanocomposite comprising PDMS elastomer and LIG nanomaterial, serving as a soft piezoresistive strain sensor capable of accommodating significant fabric deformation while preserving its natural movement. To effectively discern between various loads, we proposed a configuration featuring two sets of twin sensors: one for measuring tensile and bending deformations, and the other for measuring shear angle. We observed low cross-sensitivity of tensile and shear sensors to shear deformation (17% changes) and tensile tests (5% changes), relative to their responses in their design modes. However, both sensors exhibit a substantial sensitivity to bending deformation. Nonetheless, the tensile sensor aids in distinguishing this load from others. Consequently, by utilizing all four sensors during forming, we can potentially identify various types of loadings and their combination to defect formation, which is the next step of this research.

# 5 REFERENCES

[1] Z. T. Kier, A. Salvi, G. Theis, A. M. Waas, and K. Shahwan, "Estimating mechanical properties of 2D triaxially braided textile composites based on microstructure properties," *Composites Part B: Engineering,* vol. 68, pp. 288-299, 2015/01/01/ 2015.

[2] A. Hosseini, "A multiscale analysis of forming induced wrinkles in woven composite preforms," Text, 2018.

[3] A. Rashidi and A. S. Milani, "A multi-step biaxial bias extension test for wrinkling/de-wrinkling characterization of woven fabrics: Towards optimum forming design guidelines," *Materials & Design,* vol. 146, pp. 273-285, 2018/05/15/ 2018.

[4] B. Zhu, T. X. Yu, J. Teng, and X. M. Tao, "Theoretical Modeling of Large Shear Deformation and Wrinkling of Plain Woven Composite," *Journal of Composite Materials,* vol. 43, no. 2, pp. 125-138, 2009/01/01 2008.

[5] A. G. Prodromou and J. Chen, "On the relationship between shear angle and wrinkling of textile composite preforms," *Composites Part A: Applied Science and Manufacturing,* vol. 28, no. 5, pp. 491-503, 1997/01/01/ 1997.

[6] A. Hosseini, M. H. Kashani, F. Sassani, A. S. Milani, and F. Ko, "A Mesoscopic Analytical Model to Predict the Onset of Wrinkling in Plain Woven Preforms under Bias Extension Shear Deformation," *Materials*, vol. 10, no. 10. doi: 10.3390/ma10101184

[7] R. Bai, B. Chen, J. Colmars, and P. Boisse, "Physics-based evaluation of the drapability of textile composite reinforcements," *Composites Part B: Engineering,* vol. 242, p. 110089, 2022/08/01/ 2022.

[8] J. V. Viisainen, A. Hosseini, and M. P. F. Sutcliffe, "Experimental investigation, using 3D digital image correlation, into the effect of component geometry on the wrinkling behaviour and the wrinkling mechanisms of a biaxial NCF during preforming," *Composites Part A: Applied Science and Manufacturing,* vol. 142, p. 106248, 2021/03/01/ 2021.

[9] H. Montazerian, A. Rashidi, M. Hoorfar, and A. S. Milani, "A frameless picture frame test with embedded sensor: Mitigation of imperfections in shear characterization of woven fabrics," *Composite Structures,* vol. 211, pp. 112-124, 2019/03/01/ 2019.

[10] J. Fial, S. Carosella, L. Ring, and P. Middendorf, "Shear Characterization of Reinforcement Fabrics using Textile-applied printed Strain Sensors," *Procedia Manufacturing,* vol. 47, pp. 65-70, 2020/01/01/ 2020.

[11] R. Sourki, B. Khatir, S. S. Najar, R. Vaziri, A S. Milani, “Characterization of the dissipative large deformation bending response of dry fabric composites as occurs during forming,” *Composite Structures*, 310: 116728, 2023.